# Selective excitation enables assignment of proton resonances and 1H–1H distance measurement in ultrafast magic angle spinning solid state NMR spectroscopy

**ARTICLE** *in* THE JOURNAL OF CHEMICAL PHYSICS · JULY 2015

Impact Factor: 2.95 · DOI: 10.1063/1.4926834



**2 AUTHORS:**

Rongchun Zhang
University of Michigan
**27** PUBLICATIONS **123** CITATIONS
SEE PROFILE

Ayyalusamy Ramamoorthy
University of Michigan
**336** PUBLICATIONS **11,727** CITATIONS
SEE PROFILE

# Selective excitation enables assignment of proton resonances and 1H-1H distance measurement in ultrafast magic angle spinning solid state NMR spectroscopy

Rongchun Zhang and Ayyalusamy Ramamoorthy

Citation: The Journal of Chemical Physics **143**, 034201 (2015); doi: 10.1063/1.4926834
View online: http://dx.doi.org/10.1063/1.4926834
View Table of Contents: http://scitation.aip.org/content/aip/journal/jcp/143/3?ver=pdfcov
Published by the AIP Publishing

# Selective excitation enables assignment of proton resonances and $^{1}$H-$^{1}$H distance measurement in ultrafast magic angle spinning solid state NMR spectroscopy

Rongchun Zhang and Ayyalusamy Ramamoorthy[a)]
*Biophysics and Department of Chemistry, The University of Michigan, Ann Arbor, Michigan 48109-1055, USA*

(Received 8 May 2015; accepted 3 July 2015; published online 16 July 2015)

Remarkable developments in ultrafast magic angle spinning (MAS) solid-state NMR spectroscopy enabled proton-based high-resolution multidimensional experiments on solids. To fully utilize the benefits rendered by proton-based ultrafast MAS experiments, assignment of $^{1}$H resonances becomes absolutely necessary. Herein, we propose an approach to identify different proton peaks by using dipolar-coupled heteronuclei such as $^{13}$C or $^{15}$N. In this method, after the initial preparation of proton magnetization and cross-polarization to $^{13}$C nuclei, transverse magnetization of desired $^{13}$C nuclei is selectively prepared by using DANTE (Delays Alternating with Nutations for Tailored Excitation) sequence and then, it is transferred to bonded protons with a short-contact-time cross polarization. Our experimental results demonstrate that protons bonded to specific $^{13}$C atoms can be identified and overlapping proton peaks can also be assigned. In contrast to the regular 2D HETCOR experiment, only a few 1D experiments are required for the complete assignment of peaks in the proton spectrum. Furthermore, the finite-pulse radio frequency driven recoupling sequence could be incorporated right after the selection of specific proton signals to monitor the intensity buildup for other proton signals. This enables the extraction of $^{1}$H-$^{1}$H distances between different pairs of protons. Therefore, we believe that the proposed method will greatly aid in fast assignment of peaks in proton spectra and will be useful in the development of proton-based multi-dimensional solid-state NMR experiments to study atomic-level resolution structure and dynamics of solids.  [http://dx.doi.org/10.1063/1.4926834]

## INTRODUCTION

Though solid-state NMR spectroscopy has been a valuable technique to study a variety of non-crystalline and non-soluble chemical and biological molecules and materials, its poor sensitivity and the need for large sample quantity continue to restrict its applications.[1] Among the approaches used to enhance solid-state NMR sensitivity,[2,3] there is considerable interest in developing proton-detection based techniques that fully utilize the high natural abundance and gyromagnetic ratio of protons to enhance the sensitivity of solid-state NMR experiments.[4–9] But, unfortunately, it is difficult to obtain a high-resolution $^{1}$H NMR spectrum of a solid due to the presence of strong proton-proton dipolar couplings. The presence of a widespread dipole-coupled proton network typically results in a severe homogeneous line broadening,[10] rendering the linewidths of peaks to be much larger than proton chemical shift differences. Therefore, a combined rotation and multiple pulse spectroscopy (CRAMPS) technique has to be used to obtain a high-resolution proton spectrum with a moderate magic angle spinning (MAS) speed.[11–17] However, the windowed stroboscopic observation utilized in a CRAMPS experiment significantly increases the noise level in the spectrum.[18] In addition, the CRAMPS experimental setup is difficult, which not only places extreme demands on the speed of transmitter phase switch but also requires careful scaling of chemical shifts. On the other hand, recent developments of ultrafast MAS probes enable impressive higher spinning speeds up to 120 kHz. Furthermore, recent studies have well demonstrated the increase in spectral resolution with the spinning speed of the sample and the ability to employ proton detection in solid-state NMR experiments.[19–21] As a result, an increasing number of studies utilizing proton-detection NMR under ultrafast MAS have been reported in the recent years.[22–37] Novel pulse sequences under ultrafast MAS conditions have been demonstrated for the measurement of heteronuclear dipolar coupling and chemical shift aniosotropy.[26,38–41] The unique combination of $^{1}$H-$^{1}$H dipolar recoupling and ultrafast MAS has made proton-detected solid-state NMR methods to be quite attractive and enabled the possibility of using $^{1}$H-$^{1}$H dipolar coupling for potential structural studies.[42–45]

The ability to measure isotropic and anisotropic chemical shifts of protons by ultrafast MAS experiments will have significant impact on solid-state NMR applications. However, the proton spectrum has a narrower chemical shift range (around 20 ppm) compared to that of low-γ nuclei spectra (e.g., around 250 ppm for $^{13}$C). Therefore, the narrow chemical shift span and residual linewidths pose difficulties for the assignment of $^{1}$H resonances. This difficulty can be overcome by 2D heteronuclear correlation (HETCOR) experiments that utilize the large chemical shift span and well resolved peaks of $^{13}$C nuclei. However, 2D experiments

a)Author to whom correspondence should be addressed. Electronic mail: ramamoor@umich.edu

 

are time-consuming, especially when the sample amount is quite limited by the rotor size (generally 2–3 mg in the Agilent 1.2 mm rotor). In this study, we proposed a method for fast assignment of peaks in the $^{1}$H NMR spectrum obtained under ultrafast MAS conditions. This approach employs the DANTE (Delays Alternating with Nutations for Tailored Excitation)[46,47] sequence to selectively flip the magnetization of specific $^{13}$C nuclei after the initial $^{1}$H → $^{13}$C cross polarization (CP) period and then transfer the magnetization to bonded (or very closely located) protons for detection. Using this approach to selectively detect specific proton signals, we further demonstrate the utilization of finite-pulse radio frequency driven recoupling (fp-RFDR)[22,23,48,49] to enable magnetization transfer to the nearby protons through recoupled dipolar-couplings based spin diffusion. In this proposed approach, once the $^{13}$C resonances are assigned, which is generally easier to achieve, the proton peaks can be identified and assigned by performing a few 1D experiments. Moreover, the relative distances between different pairs of protons could be determined. Therefore, the pulse sequence proposed in this study could provide abundant information about proton resonance assignments and $^{1}$H-$^{1}$H distances and will be beneficial for the understanding and interpretations of proton-based multidimensional solid-state NMR spectra.

## EXPERIMENTS

### Material

Uniformly, $^{13}$C,$^{15}$N-labeled L-alanine sample was purchased from Isotec (Champaign, IL) and $^{13}$C,$^{15}$N-labeled L-histidine·HCl·$H_2O$ sample was purchased from Acros Organics (Morris Plains, NJ). All samples were used as received without any further purification.

### Pulse sequences

All NMR experiments were performed on an Agilent VNMRS 600 MHz solid-state NMR spectrometer equipped with a triple-resonance 1.2 mm MAS probe. About 2–3 mg of samples were used in the 1.2 $\mu$l volume rotor. A 60 kHz MAS speed was used for all experiments in this study. The RF pulse sequences used in this study are shown in Fig. 1. After the 90° preparation pulse, the $^{1}$H transverse magnetization is transferred to $^{13}$C nuclei using ramped cross polarization,[50] and then, the $^{13}$C transverse magnetization is stored along the $z$-axis while the phase-alternated HORROR sequence[51] is applied to destroy the $^{1}$H magnetization remaining after CP. Following this, the DANTE sequence is used to selectively flip the desired $^{13}$C magnetization onto the transverse plane, and then, the selected $^{13}$C magnetization is transferred to bonded protons for detection with a short-contact-time CP. Although a refocused-insensitive nuclei enhanced by polarization transfer (RINEPT)[52,53] can also be used for magnetization transfer in rigid solids under ultrafast MAS conditions, it requires the presence of both $^{1}$H-$^{1}$H and $^{13}$C-$^{1}$H dipolar couplings as demonstrated in our previous study;[53] however, the RINEPT-based magnetization transfer requiring a long total evolution time (generally >0.6 ms) may unavoidably result in the $^{1}$H-$^{1}$H spin diffusion during the $^{13}$C → $^{1}$H magnetization transfer process. As a result, the non-bonded protons could also gain signals from the nearby protons due to spin diffusion resulting from the residual/unaveraged $^{1}$H-$^{1}$H dipolar couplings. Besides, CP has higher polarization transfer efficiency than RINEPT. Thus, CP is preferred over RINEPT in the pulse sequence. As long as a short contact time is used, the effect of $^{1}$H-$^{1}$H spin diffusion could be ignored. For the ramped-CP, a RF field strength of 120 kHz on the $^{1}$H channel with a 20% ramp ratio and 180 kHz on $^{13}$C channel was used. The contact time for the first CP was 2–5 ms, while it was 50–100 $\mu$s

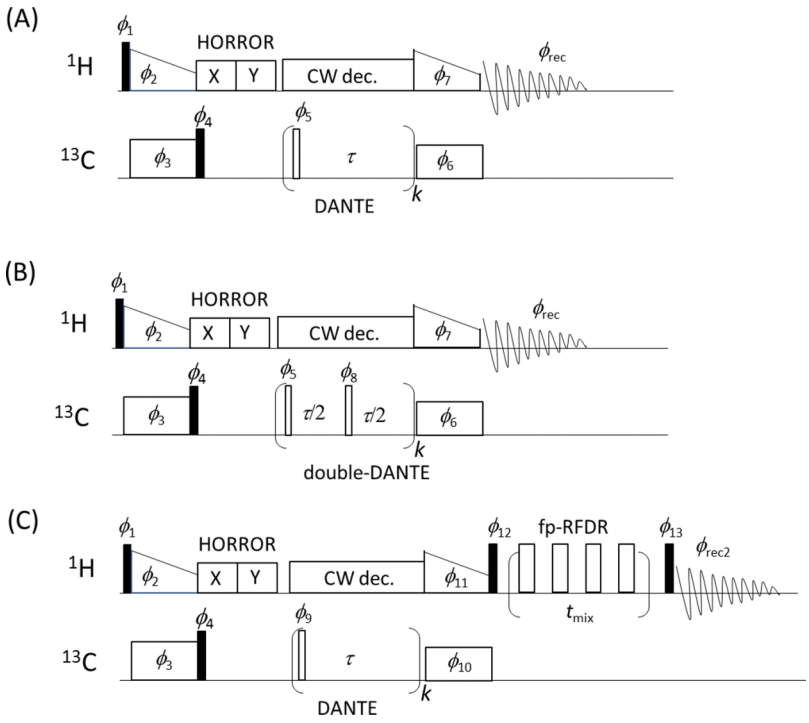


FIG. 1. RF pulse sequences for selective detection of proton resonances. Schematic representation of the pulse sequence used in this study for selective observation of proton signal with (a) singly selective DANTE, (b) doubly selective DANTE, and (c) singly selective DANTE and fp-RFDR on the $^{13}$C and $^{1}$H channel, respectively. The black solid rectangle is a 90° pulse and the wide blank rectangles in fp-RFDR are 180° pulses. The small flip angle of the short pulse in DANTE sequence is $\pi/(2k)$. The phase cycling schemes are: $\phi_1 = 1111$, $\phi_2 = 0000$, $\phi_3 = 0000$, $\phi_4 = 1111$, $\phi_5 = 0202$, $\phi_6 = 1111$, $\phi_7 = 0011$, $\phi_{rec} = 0213$, $\phi_9 = 0000$, $\phi_{10} = 1111$, $\phi_{11} = 1313$, $\phi_{12} = 0022\ 0022$, $\phi_{13} = 0000\ 2222\ 2222\ 0000$, and $\phi_{rec2} = 0220\ 2002\ 2002\ 0220$. In the double-DANTE sequence, $\phi_8$ is phase incremented during the repetition of the interleaved two pulses to make sure that at the end of DANTE, $\phi_8 = \phi_5$.

for the second CP in order to avoid proton diffusion as well as the $^{13}C \rightarrow {}^{1}H$ magnetization transfer to remote protons. $^{1}H$ 90° pulse width was 1.4 $\mu$s and a 3 $\mu$s 90° pulse was used for $^{13}C$. A low RF power (~24 kHz) CW (Continuous-Wave) decoupling was used during DANTE excitation. Recycle delays used for experiments on alanine and histidine samples were 3 and 10 s, respectively.

In the DANTE sequence, the flip angle of the pulse, θp, is equal to $\pi/(2k)$. In all the experiments, $k$ was around 15. In the singly selective DANTE sequence (in Fig. 1(a)), the inter-pulse delay, $\tau$, was set to one rotor period to make sure that the DANTE sideband is out of the observed spectral frequency range. In the doubly selective DANTE sequence (in Fig. 1(b)), $\tau = \frac{\Delta\phi}{360\Delta\delta}$, where $\Delta\phi$ is the phase increment of the second pulse during the repetition period of the two interleaved flip pulses, and $\Delta\delta$ is the resonance frequency difference for the two selective $^{13}C$ peaks. $\Delta\phi$ was chosen such that at the end of the double-DANTE sequence, the phase of the two interleaved pulses was the same, i.e., $\phi_8 = \phi_5$. For the fp-RFDR sequence, the $XY4^{1}_{4}$ phase cycling scheme was used for the 180° pulse, which was demonstrated to have the best performance for recoupling $^{1}H$-$^{1}H$ dipolar couplings and enabling efficient magnetization transfer under ultrafast MAS conditions.[22,23] Before the acquisition of spectra using the proposed pulse sequence, as part of the experimental setup process, the contact time of second $^{13}C \rightarrow {}^{1}H$ CP was set to zero to make sure the complete suppression of proton magnetization remaining in the proton channel before the signal acquisition and to confirm that all the detected proton signals come via the second CP step. It should be mentioned that the shaped pulses, mostly Gaussian pulses,[54] that exhibit a better performance than DANTE could be used for frequency-selective excitation. However, DANTE is much easier to set up in any NMR spectrometer.

### Simulations

The numerical simulation of $^{13}C \rightarrow {}^{1}H$ CP efficiency was performed using the SIMPSON software.[55,56] A $C_2H_4$ (consisting of CH and $CH_3$ groups) spin system was used with coordinates taken from the crystal structure of L-alanine.[57] $^{13}C$-$^{1}H$ dipolar couplings of 22.8 and 7.6 kHz were used for CH and $CH_3$ groups, respectively. Only the isotropic chemical shifts of $^{13}C$ nuclei were considered, while isotropic chemical shifts and the chemical shift anisotropy (CSA) as well as the $J$ couplings of protons were neglected. All $^{1}H$-$^{1}H$ and $^{13}C$-$^{1}H$ dipolar couplings are also taken into consideration. RF field strengths of 120 and 180 kHz on the $^{1}H$ and $^{13}C$ channels, respectively, were used for the magnetization transfer. Magnetizations of all protons were determined during the CP process, where the initial $^{13}C$ magnetization was either from the $CH_3$ or CH group.

The proton spin diffusion through fp-RFDR under 60 kHz MAS was also simulated using SIMPSON,[55,56] where the proton spin system was modeled according to the crystal structure of L-histidine·HCl·$H_2O$.[58] Only $^{1}H$-$^{1}H$ dipolar couplings were considered for the polarization transfer efficiency. The 180° pulse length used in simulations was the same as that in experiments. In order to quantitatively compare the polarization efficiencies, the longitudinal magnetization buildup rate was defined as the inverse of the mixing time needed to reach the maximum magnetization transfer.

## RESULTS AND DISCUSSION

Assignment of resonances in high-resolution proton spectra obtained under ultrafast MAS is beneficial for the accurate interpretations of proton-detected multidimensional solid-state NMR experiments and also to get detailed information about molecular structures and dynamics. In this study, we demonstrate some simple RF pulse sequences to identify the chemical shifts of protons bonded to different carbons by using frequency-selective DANTE sequences in the $^{13}C$ channel.

Uniformly $^{13}C$–$^{15}N$-labeled L-alanine sample is used as the model system in this study. Experimental results demonstrating the selective detection of chemically different protons are shown in Fig. 2. By using the singly selective DANTE excitation pulse sequence shown in Fig. 1(a), proton

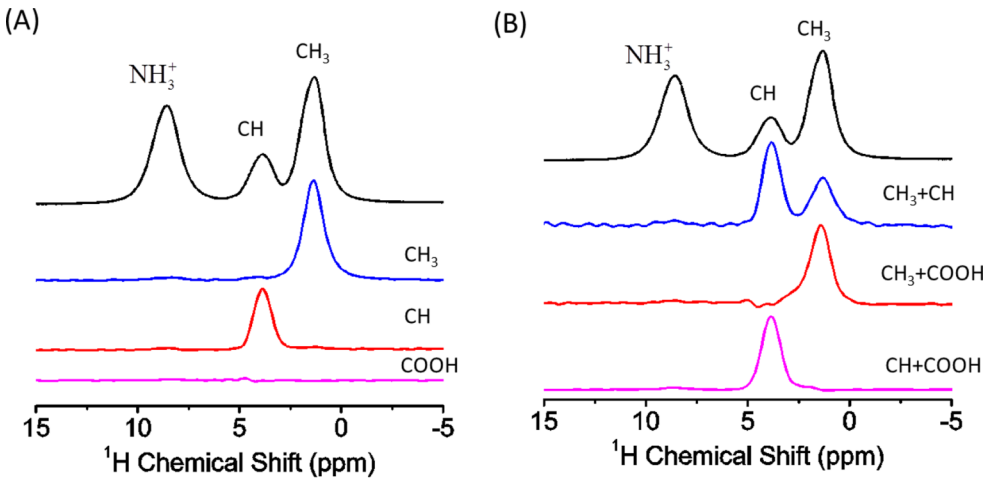


FIG. 2. Selective detection of proton resonance under ultrafast MAS frequencies. Selective observation of proton resonances from L-alanine obtained using (a) singly selective DANTE and (b) doubly selective DANTE excitations of $^{13}C$ peaks of the indicated chemical groups under 60 kHz MAS. The full $^{1}H$ spectrum of L-alanine obtained from a single pulse excitation at 60 kHz MAS is shown at the top. Each spectrum was the resultant of the co-addition of 8 scans.

signals from $CH_3$ and CH groups could be easily identified. Since a short contact time was used in the second $^{13}C \rightarrow {}^{1}H$ CP, the $^{13}C$ magnetization is transferred only to directly bonded protons. It is remarkable that the spectra in Fig. 2(a) are highly selective to either the CH or $CH_3$ group. As shown in Fig. 2(a), no proton signals were detected if DANTE was used to selectively flip the $^{13}C$ magnetization of the carboxyl group. Similarly, as experimentally demonstrated in Fig. 2(b), by using the pulse sequence (shown in Fig. 1(b)) that employs doubly selective DANTE, two desired $^{13}C$ peaks that differ in chemical shift values are selectively flipped and, therefore, the proton signals corresponding two different chemical groups can be identified. Due to the absence of a bonded proton in the carboxyl group of alanine, only one proton peak was observed when the $^{13}C$ signals of CH and $COO^-$ or $CH_3$ and $COO^-$ were selectively flipped using the doubly selective DANTE sequence. The experimental results shown in Fig. 2 clearly demonstrate the robust performance of the proposed pulse sequences for an efficient identification of peaks in the proton spectrum.

Though the resolution in proton spectra depends on the spinning speed as demonstrated in previous studies,[20,21] to a large extent, the efficiency of the DANTE sequence determined the ability of the pulse sequences to selectively observe proton signals under ultrafast MAS conditions. In addition, it is important to note that the second $^{13}C \rightarrow {}^{1}H$ CP step in the pulse sequence also plays a very important role, as the remote weak $^{13}C \rightarrow {}^{1}H$ dipolar couplings could also result in non-bonded $^{13}C \rightarrow {}^{1}H$ magnetization transfer. Besides, the $^{1}H$-$^{1}H$ spin diffusion induced by the unsuppressed $^{1}H$-$^{1}H$ dipolar couplings during the CP process may also affect the final selectivity of proton signals. However, the spin diffusion effect can be neglected as long as the CP contact time is kept short, because the ultrafast MAS frequency has greatly suppressed the $^{1}H$-$^{1}H$ dipolar couplings.

To fully understand the performance of the pulse sequences, numerical simulations were performed to examine the $^{13}C \rightarrow {}^{1}H$ CP efficiency for CH and $CH_3$ groups by using a $C_2H_4$ spin system as described in the Simulations section above. As shown in Fig. 3, when the $^{13}C$ signal of the CH group was selected for the $^{13}C \rightarrow {}^{1}H$ polarization transfer (case A), the CH proton signal build up quickly due to the fast magnetization transfer via the strong $^{13}C$-$^{1}H$ dipolar coupling. However, the methyl proton signal also slowly builds up due to the presence of remote $^{13}C$-$^{1}H$ dipolar couplings (which is ~3.0 kHz). The methyl proton signal intensity becomes comparable to that of the CH group for a 1 ms contact time. The situation is quite different when the $^{13}C$ signal of the $CH_3$ group was selected for the $^{13}C$-$^{1}H$ magnetization transfer (case B). Even for a 1 ms contact time, the methyl proton signal intensity is still much larger than that of the CH group proton signal, although the remote $^{13}C$-$^{1}H$ dipolar coupling (~3.0 kHz) is the same as that in case A. This difference between cases A and B is attributed to the difference in the number of remote protons. Indeed, the $CH_3$ proton signal intensity in case A is three times that of the CH proton signal intensity in case B, as there are three remote protons ($CH_3$) for case A, whereas only one (CH) for case B.

For an isolated $^{13}C$-$^{1}H$ spin pair (denoted as $S$-$I$), the transferred CP signal at a contact time $\tau$ is given as[59]

$$S(\tau) = -\frac{\varepsilon\gamma_S}{2\gamma_I}\left(\frac{b_n^2}{b_n^2+\Delta v_n^2}\right)[1-\cos(\tau(b_n^2+\Delta v_n^2)^{1/2})], \quad (1)$$

where $\varepsilon = 1$ for double-quantum CP or $\varepsilon = -1$ for zero-quantum CP according to the Hartmann-Hahn matching condition, $w_{eS} + \varepsilon w_{eI} \approx nw_R (n = \pm 1, \pm 2)$. $w_{eI} = \sqrt{w_{1I}^2 + \Delta w_I^2}$ and $w_{eS} = \sqrt{w_{1S}^2 + \Delta w_S^2}$ are the effective RF field strengths on $I$ and $S$ spins, respectively; $w_{1S}$ and $w_{1I}$ are the spin-lock RF strengths used on $^{13}C$ and $^{1}H$ channels, respectively, during CP; $\Delta w_I$ and $\Delta w_S$ are the chemical shift resonance offsets for $I$ and $S$ spins, respectively; $w_R$ is the spinning speed and $\Delta v_n = w_{1S} + w_{1I} - nw_R$. $\gamma_S$ and $\gamma_I$ are the gyromagnetic ratios of $^{13}C$ and $^{1}H$ nuclei, respectively.

For different matching conditions (as defined by $n = \pm 1, \pm 2$), the term $b_n$ can be written as follows:

$$b_{\pm 1} = \frac{\gamma_I\gamma_S\hbar}{2\sqrt{2}r^3}\sin 2\beta, \quad (2a)$$

$$b_{\pm 2} = \frac{\gamma_I\gamma_S\hbar}{4r^3}\sin^2\beta, \quad (2b)$$

where $\beta$ is the angle between the internuclear vector and the MAS rotor axis. For a very short CP contact time (e.g., 50 $\mu$s), $\tau(b_n^2 + \Delta v_n^2)^{1/2} << 1$ because the heteronuclear

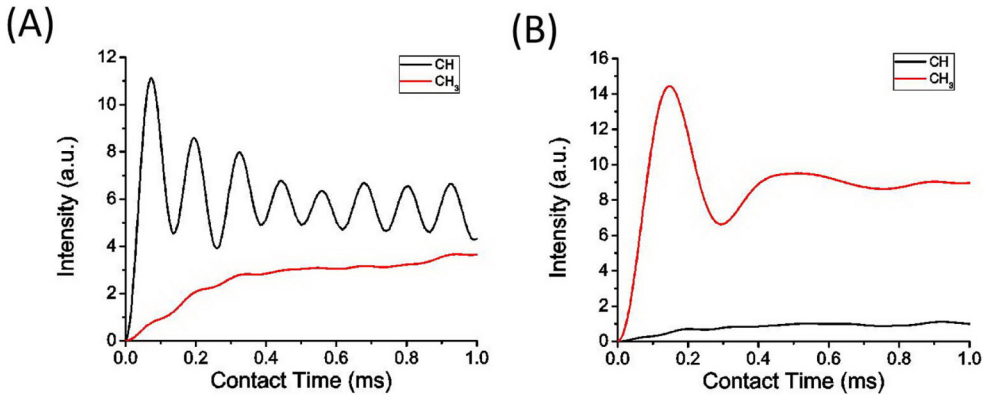


FIG. 3. Simulated $^{13}C \rightarrow {}^{1}H$ cross-polarization transfer efficiencies. $^{13}C$ peak of CH (a) or $CH_3$ (b) group was selected for $^{13}C \rightarrow {}^{1}H$ magnetization transfer. The transferred transverse magnetizations of protons from both chemical groups were quantified in each case. All simulations were carried out using the SIMPSON software as explained in the main text.

dipolar coupling constant $D_{CH} = -\frac{\mu_0 \gamma_I \gamma_S \hbar}{4r^3\pi}$ is large (generally a few kHz). Therefore, Eq. (1) becomes

$$S(\tau) = -\frac{\varepsilon\gamma_S}{2\gamma_I}\left(\frac{b_n^2}{b_n^2+\Delta v_n^2}\right)[1-\cos(\tau(b_n^2+\Delta v_n^2)^{1/2})]$$
$$\sim -\frac{\varepsilon\gamma_S}{2\gamma_I}\left(\frac{b_n^2}{(b_n^2+\Delta v_n^2)^{1/2}}\right)\tau. \quad (3)$$

As a result, when there is no Hartmann-Hahn mismatch, $\Delta v_n = 0$, the CP signal intensity becomes

$$S(\tau) \sim -\frac{\varepsilon\gamma_S}{2\gamma_I} b_n \tau. \quad (4)$$

Therefore, the CP signal intensity is proportional to $b_n$, i.e., the heteronuclear $^{13}$C-$^{1}$H dipolar coupling constant. Because of this relationship, a stronger heteronuclear dipolar coupling will result in a faster signal buildup in a cross-polarization experiment.

Though the intensity of a signal obtained via CP depends on the magnitude of the heteronuclear dipolar coupling as explained above, the contact time for the second $^{13}$C → $^{1}$H CP should be as small as possible in order to avoid the CP between the selected carbon and the remote protons as well as to avoid spin diffusion induced by the residual $^{1}$H-$^{1}$H dipolar couplings. Generally, as indicated in Fig. 3, the contact time for the second CP should be kept below 0.1 ms so that the remote $^{13}$C → $^{1}$H polarization transfer could be reasonably neglected. However, this value should be optimized depending on the experimental conditions, particularly the spinning speed of the sample. If the sample is not $^{13}$C enriched, a longer contact time (up to ~0.5 ms) could be used as demonstrated in proton-detected HETCOR experiments.[60–63]

The performances of these pulse sequences were further examined on a uniformly $^{13}$C,$^{15}$N-labeled L-histidine·HCl·$H_2O$ powder sample and the results are shown in Fig. 4. The $^{13}$C CPMAS NMR spectrum obtained at 60 kHz MAS is shown in Fig. 4(b). Unlike the proton spectrum of alanine, the proton spectrum of L-histidine·HCl·$H_2O$ is not well resolved; peaks from H1 and H2 overlap and peaks from H3, H5, and H7 are not well resolved. On the basis of the $^{13}$C spectrum, we were able to identify the resonance frequency for each proton in L-histidine·HCl·$H_2O$. As shown in Fig. 4(c), protons bonded to each carbon can be identified using the singly selective DANTE excitation pulse sequence. It is remarkable that even the completely overlapping proton peaks from H1 of the $CH_2$ and H2 of the CH are selectively acquired. The resultant spectra reveal that the linewidth of H1 peak is broader than that of H2, indicating that H1 experiences stronger unsuppressed $^{1}$H-$^{1}$H dipolar couplings than that of H2. This observation is

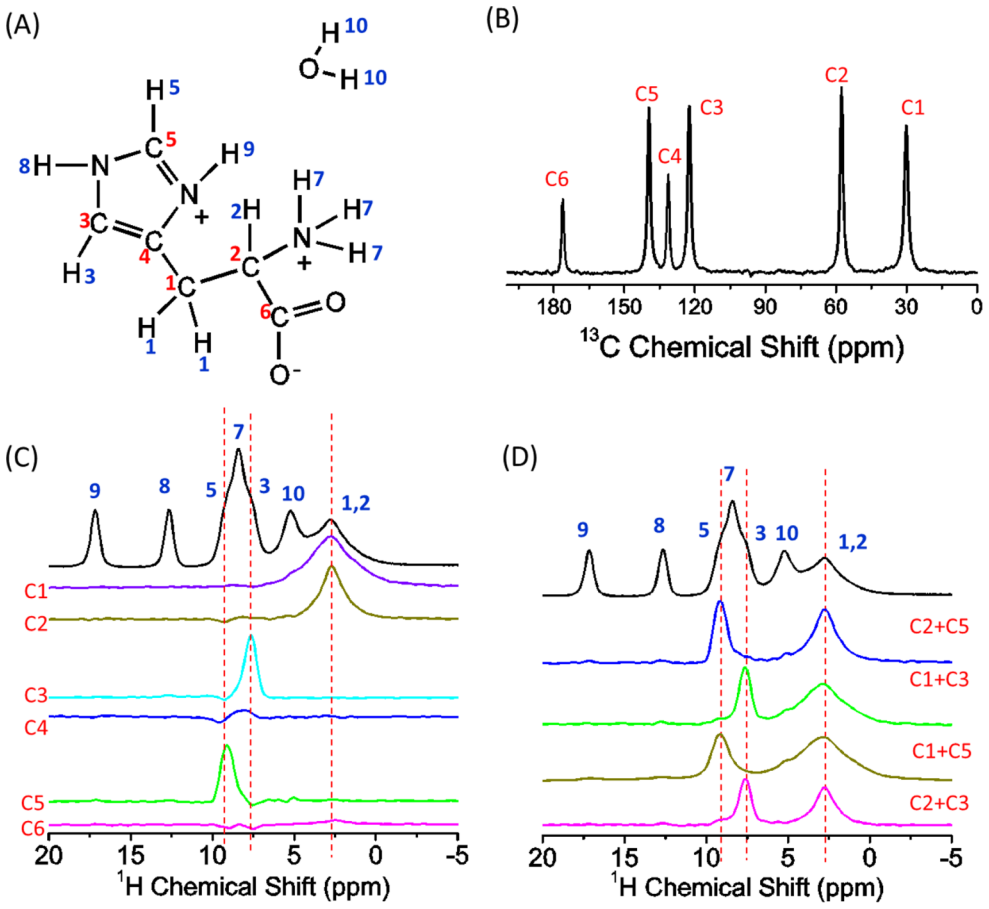


FIG. 4. Selective detection of single or two different proton resonances under ultrafast MAS frequencies. (a) Molecular structure of L-histidine · HCl · $H_2O$. (b) $^{13}$C CPMAS spectrum of L-histidine · HCl · $H_2O$ under 60 kHz MAS. (c) Selective observation of single proton resonance by using singly selective DANTE excitation (given in Fig. 1(a)). (d) Selective observation of resonances from two chemically different protons by using doubly selective DANTE excitation sequence (given in Fig. 1(b)) on chemically different $^{13}$C nuclei as indicated. The single pulse $^{1}$H spectrum is shown at the top in (c). Each spectrum was obtained by co-adding 8 scans.

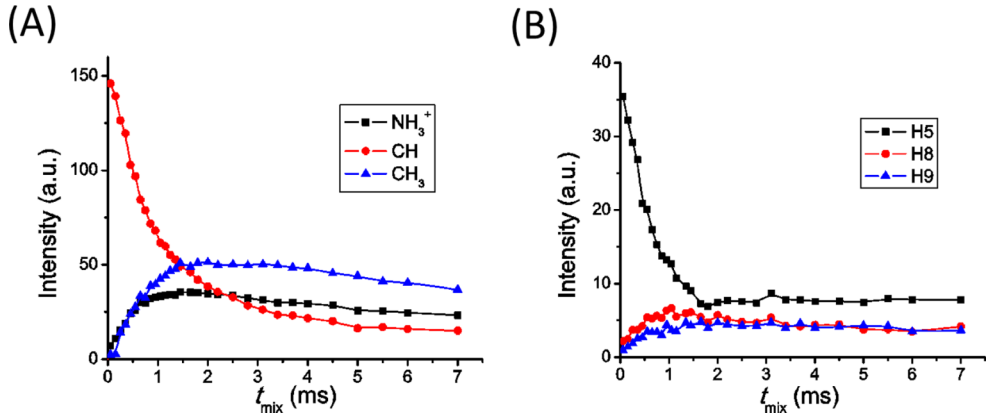


FIG. 5. Selective monitoring of $^1H/^1H$ magnetization exchange under ultrafast MAS frequencies. Selective observation of proton signal intensity using the sequence shown in Fig. 1(c) for L-alanine (a) and L-histidine·HCl·$H_2O$ (b) under 60 kHz MAS. (a) Decay of CH proton peak intensity and intensity buildup of $NH_3^+$ and $CH_3$ peaks as a function of fp-RFDR mixing time following the selective excitation of CH peak in L-alanine. (b) Decay of H5 peak intensity and intensity buildup of H8 and H9 peaks as a function of fp-RFDR mixing time following the selective excitation of H5 peak in L-histidine·HCl·$H_2O$. 32 and 64 scans were acquired for alanine and histidine samples, respectively, for each mixing time.

understandable because there are two H1 protons bonded to C1, whereas only one proton (H2) is bonded to C2. These results suggest that the proposed pulse sequence and the approach could be used to measure the dynamics (or the time scale of motion) of different chemical groups in a molecule or the difference in the dynamics of different chemical components in a heterogeneous sample by measuring the linewidths for proton peaks. Though similar information could be determined from 2D WISE (wideline separation) experiments,[64] our proton-based approach is much faster as 2D WISE data collection typically takes more than a day. It is also remarkable that the spectra shown in Fig. 4 reveal that protons H3 and H5 bonded to C3 and C5, respectively, exhibit different chemical shift values, whereas the H3 and H5 peaks are overlapped with the peak from H7 in the single pulse proton spectrum. Therefore, our experimental results demonstrate that by the selective acquisition of H1–H5 resonances, based on the selective excitation of $^{13}C$ peaks, we were able to identify the overlapping proton peaks that are generally difficult to distinguish in a single pulse proton spectrum. Results presented in Fig. 4 also reveal no proton signals for DANTE excitation of C4 or C6 resonance, indicating that there are no protons bonded to C4 or C6.

As shown in Fig. 4(d), the doubly selective DANTE sequence is useful to selectively detect signals from protons bonded to two chemically different carbons at the same time. Each 1D spectrum exhibits only two peaks corresponding to two of the desired protons in the molecule. The overlapped peaks from H1 and H2, as well as from H3 and H5, can be clearly distinguished.

On the basis of the selective detection of specific proton peaks, we could further study the effect of spin diffusion between the selected protons and the nearby ones by using the pulse sequence shown in Fig. 1(c). The pulse sequence uses fp-RFDR to recouple $^1H$-$^1H$ dipolar couplings that enable the exchange of longitudinal magnetization between different protons in the system. This can be thought as an inverse process to the well-known "*hole-burning*" experiment for the measurement of spin diffusion coefficient.[65] In a *hole-burning* experiment, a specific resonance frequency is first quenched and then, the intensity buildup of the quenched resonance due to magnetization exchange through spin diffusion is monitored to determine the spin diffusion coefficient. The efficiency of the pulse sequence (given in Fig. 1(c)) is experimentally demonstrated and the results are shown in Fig. 5. For the L-alanine sample, the proton peak of the CH group was selected as demonstrated before, and then, the intensities of proton peaks of $CH_3$ as well as $NH_3^+$ groups were measured as a function of fp-RFDR mixing time. The similar buildup rates observed for $CH_3$ and $NH_3^+$ peaks indicate that proton-proton distances in CH–$CH_3$ and CH–$NH_3^+$ groups are similar. However, the protons in the $NH_3^+$ group experience stronger dipolar couplings with the surrounding protons, which result in a fast relay of spin diffusion and thus a rapid signal decay as shown by the experimental results in Fig. 5. Similar experiments were also performed on L-histidine·HCl·$H_2O$, where the magnetization of H5 proton was selectively prepared for fp-RFDR mixing and intensity buildups for H8 and H9 protons were measured. As shown in Fig. 5(b), the buildup rate measured for H8 peak is slightly faster than that for H9 peak, indicating a closer distance between H5 and H8 (~2.38 Å) than that between H5 and H9 (~2.46 Å). This experimental result is in good agreement with the crystal structure of L-histidine·HCl·$H_2O$.[58] It should be noted here that only the initial signal intensity buildup rates measured from experiments are useful in determining inter-proton distances.

As demonstrated in a previous experimental ultrafast MAS solid-state NMR study,[23] the fp-RFDR enabled rate of magnetization buildup increases with the magnitude of $^1H$-$^1H$ dipolar coupling. Therefore, it should be technically feasible to determine $^1H$-$^1H$ distances based on the relationship between buildup rate and dipolar couplings. In this study, utilizing SIMPSON based numerical simulations and the parameters used in the experiments, the magnetization transfer efficiency was calculated for a two-spin system. Simulated results are shown in Fig. 6(a), and the magnetization buildup rate ($R$) dependence on $^1H$-$^1H$ dipolar couplings was fitted to a linear function given below

$$R = 0.107^{*}D_{HH} - 8.63, \quad (5)$$

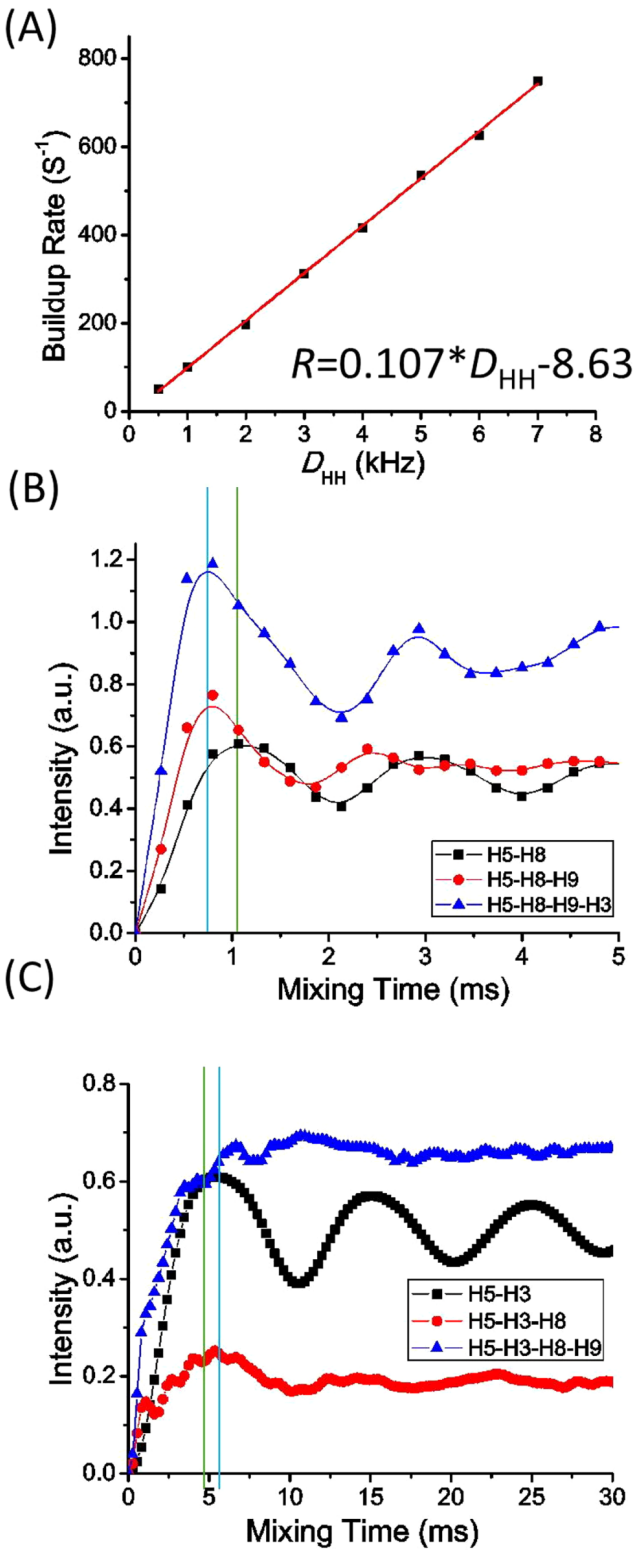


FIG. 6. Determination of $^1$H-$^1$H distances from solids. (a) Simulated buildup rate ($R$) as a function of the $^1$H-$^1$H dipolar couplings ($D_{HH}$) in a two-spin system. The buildup rate increases linearly with the magnitude of $^1$H-$^1$H dipolar coupling. ((b) and (c)) $^1$H/$^1$H magnetization transfer through proton-proton dipolar couplings recoupled by fp-RFDR under 60 kHz MAS was obtained experimentally (Fig. 5) and also simulated using SIMPSON. Simulated H5 → H8 (b) and H5 → H3 (c) polarization transfer efficiencies using different model proton spin systems as indicated. The green and cyan vertical lines indicate the mixing time corresponding to the maximum transfer in two-spin and three-spin (and four-spin) systems, respectively. The proton spin systems used in the simulations were modeled based on the crystal structure of L-histidine · HCl · $H_2O$.

where

$$D_{HH} = -\frac{\mu_0 \hbar \gamma^2}{4r^3\pi}. \quad (6)$$

$\gamma$ is the gyromagnetic ratio of proton and $r$ is the proton-proton distance. As determined from the experimental data given in Fig. 5(b), the H5-H8 and H5-H9 buildup rates are 1000 and 884.9 Hz, respectively. Using these experimentally measured buildup rates, the H5-H8 and H5-H9 distances determined from Equations (5) and (6) are to be around 2.33 Å and 2.43 Å, respectively. These distances are in very good agreement with the crystal structure.[58]

In order to test the accuracy of the two-spin model used above and to understand the effect of multi-spin dipolar couplings on the experimentally measured buildup rate, H5 → H8 (Fig. 6(b)) and H5 → H3 (Fig. 6(c)) magnetization transfers were numerically simulated with different number of protons nearby. In Fig. 6(b), H5-H8 dipolar coupling is stronger than other $^1$H-$^1$H dipolar couplings in the H5-H8-H9 and H5-H8-H9-H3 spin systems, while in Fig. 6(c), the H5-H3 dipolar coupling is much weaker than other dipolar couplings in H5-H3-H8 and H5-H3-H8-H9 systems. As expected, the presence of multiple dipolar couplings did slightly increase the buildup rate when H5-H8 dipolar coupling is dominant for the H5 → H8 polarization transfer (Fig. 6(b)), whereas the buildup rate slightly decreases when H5-H3 dipolar coupling is weaker than other $^1$H-$^1$H dipolar couplings due to dipolar truncation[66] (Fig. 6(c)). In fact, the buildup rate is the same for the three-spin and four-spin systems. Nevertheless, these small differences in the buildup rates for two and three-spin (as well as four-spin) systems did not significantly change the proton-proton distance determined from the $R$ vs $D_{HH}$ curve (Fig. 6(a)) generated from Eq. (5). For example, in Fig. 6(b), when the buildup time changes from 1.1 to 0.8 ms, the extracted $^1$H-$^1$H distance changes from 2.41 Å to 2.17 Å, whereas in Fig. 6(c), when the buildup time changes from 4.5 to 5.9 ms, the extracted $^1$H-$^1$H distance changes from 3.82 Å to 4.16 Å. Therefore, the deviation from the measured $^1$H-$^1$H distance value is only around ±0.3 Å, which is reasonable. Overall, the accurate determination of the buildup rate is the key to determine $^1$H-$^1$H distances from solids. Since fp-RFDR is a first-order recoupling pulse sequence, for a weakly dipolar coupled pair of protons that are strongly coupled with another proton, dipolar truncation effect[60,66] will be significant, which would affect the determination of $^1$H-$^1$H distances.

Although $^{13}$C-labelled samples are used in this study, the proposed experiments can also be applied to unlabeled samples. Indeed, proton-detected HETCOR experiment[62,63] under ultrafast MAS has been demonstrated for studies on unlabeled molecules. It is remarkable that a high quality spectrum generally could be obtained within a few hours, even in a 0.75 mm rotor (~290 nl sample volume).[63] In fact, our proposed pulse sequence is similar to the proton-detected HETCOR experiment. Since the DANTE sequence does not result in a significant signal loss for the selected $^{13}$C magnetization, our pulse sequences should approximately have the same signal-to-noise ratio as the proton-detected HETCOR experiment under ultrafast MAS, or even higher for some cases because there is no $^{13}$C chemical shift evolution

(for the selected $^{13}C$ sites) before the polarization transfer to $^{1}H$ for detection. Therefore, we believe that our method would also be applicable for unlabeled samples. It may also be noted that a complete assignment of $^{1}H$ resonances in systems with a lot of $^{13}C$ sites, our selective excitation method may be less advantageous compared to a 2D HETCOR experiment. Nevertheless, our method would be valuable for small molecular compounds including polymorphic pharmaceuticals for whose analyses solid-state NMR has already become an inevitable technique. Finally, as experimentally demonstrated in this study, by using a selective excitation method in our pulse sequence, we are able to specifically select the magnetization of certain proton spins. Following this, the evolution of proton magnetization can be further controlled by spin diffusion to homonuclear/heteronuclear spin pairs, and thus enabling distance measurements between specific homonuclear/heteronuclear spin pairs. As demonstrated in this study, by incorporating fp-RFDR mixing after the selection of a specific proton magnetization, $^{1}H$-$^{1}H$ distances could be determined with the help of numerical simulations of experimental results.

## CONCLUSION

In this study, we have experimentally demonstrated an approach to selectively observe resonance peaks from chemically different protons under ultrafast MAS conditions. Our experimental results successfully demonstrate that the proposed pulse sequences effectively utilize singly or doubly selective DANTE on $^{13}C$ to select only the desired $^{13}C$ peaks, whose magnetization is transferred to bonded protons by a short-contact-time CP, for a selective detection of protons and thus enabling resonance assignment. The experimental results from L-alanine and L-histidine·HCl·$H_2O$ clearly demonstrate the robust performances of the proposed sequences. Furthermore, utilizing such selective excitation and observation, the overlapped proton signals can also be distinguished. Finally, by incorporating fp-RFDR sequence after the selection of specific protons resonance, the nearby proton peak intensity could be monitored as a function of fp-RFDR mixing time, on the basis of which, we further proposed a simple approach to determine $^{1}H$-$^{1}H$ distances using numerical simulations. Overall, the pulse sequences are simple, robust, and quite easy to setup, and therefore will be useful for the interpretation of multi-dimensional proton-based solid-state NMR spectra. While the proposed techniques may have limitations for studies on large-size molecules like proteins, the use of selectively labeling with a combination of $^{13}C$, $^{15}N$, and $^{2}H$ isotopes would effectively utilize the values of the techniques under ultrafast-MAS conditions. Therefore, we believe that the approach and results reported in this study will be useful in the development of techniques to overcome the difficulties posed by spectral resolution and resonance assignment in proton spectra obtained under ultrafast MAS conditions.

## ACKNOWLEDGMENTS

This study was supported by funds from National Institutes of Health (GM084018 and GM095640 to A.R.).

[1]T. Fujiwara and A. Ramamoorthy, Annu. Rep. NMR Spectrosc. **58**, 155 (2006).
[2]R. Tycko, Acc. Chem. Res. **46**, 1923 (2013).
[3]T. Maly, G. T. Debelouchina, V. S. Bajaj, K.-N. Hu, C.-G. Joo, M. L. Mak–Jurkauskas, J. R. Sirigiri, P. C. A. van der Wel, J. Herzfeld, R. J. Temkin, and R. G. Griffin, J. Chem. Phys. **128**, 052211 (2008).
[4]D. H. Zhou, G. Shah, M. Cormos, C. Mullen, D. Sandoz, and C. M. Rienstra, J. Am. Chem. Soc. **129**, 11791 (2007).
[5]D. H. Zhou, J. J. Shea, A. J. Nieuwkoop, W. T. Franks, B. J. Wylie, C. Mullen, D. Sandoz, and C. M. Rienstra, Angew. Chem., Int. Ed. **46**, 8380 (2007).
[6]D. H. Zhou, G. Shah, C. Mullen, D. Sandoz, and C. M. Rienstra, Angew. Chem. **121**, 1279 (2009).
[7]V. Chevelkov, K. Rehbein, A. Diehl, and B. Reif, Angew. Chem., Int. Ed. **45**, 3878 (2006).
[8]R. Bernd, J. Magn. Reson. **216**, 1 (2012).
[9]S. Asami and B. Reif, Acc. Chem. Res. **46**, 2089 (2013).
[10]M. M. Maricq and J. S. Waugh, J. Chem. Phys. **70**, 3300 (1979).
[11]E. Vinogradov, P. K. Madhu, and S. Vega, Chem. Phys. Lett. **314**, 443 (1999).
[12]M. Mehring and J. S. Waugh, Phys. Rev. B **5**, 3459 (1972).
[13]M. H. Levitt, A. C. Kolbert, A. Bielecki, and D. J. Ruben, Solid State Nucl. Magn. Reson. **2**, 151 (1993).
[14]D. Sakellariou, A. Lesage, P. Hodgkinson, and L. Emsley, Chem. Phys. Lett. **319**, 253 (2000).
[15]D. P. Burum and W. K. Rhim, J. Chem. Phys. **71**, 944 (1979).
[16]M. H. Levitt, "Symmetry-based pulse sequences in magic-angle spinning solid-state NMR," in *eMagRes* (John Wiley & Sons, Ltd., 2007).
[17]J.-P. Amoureux, B. Hu, and J. Trébosc, J. Magn. Reson. **193**, 305 (2008).
[18]D. H. Zhou, "Fast magic angle spinning for protein solid-state NMR spectroscopy," in *eMagRes* (John Wiley & Sons, Ltd., 2010).
[19]S. Parthasarathy, Y. Nishiyama, and Y. Ishii, Acc. Chem. Res. **46**, 2127 (2013).
[20]Y. Nishiyama, Y. Endo, T. Nemoto, H. Utsumi, K. Yamauchi, K. Hioka, and T. Asakura, J. Magn. Reson. **208**, 44 (2011).
[21]A. Samoson, T. Tuherm, and Z. Gan, Solid State Nucl. Magn. Reson. **20**, 130 (2001).
[22]Y. Nishiyama, R. Zhang, and A. Ramamoorthy, J. Magn. Reson. **243**, 25 (2014).
[23]R. Zhang, Y. Nishiyama, P. Sun, and A. Ramamoorthy, J. Magn. Reson. **252**, 55 (2015).
[24]A. K. Chattah, R. Zhang, K. H. Mroue, L. Y. Pfund, M. R. Longhi, A. Ramamoorthy, and C. Garnero, Mol. Pharmaceutics **12**, 731 (2015).
[25]K. H. Mroue, R. Zhang, P. Zhu, E. McNerny, D. H. Kohn, M. D. Morris, and A. Ramamoorthy, J. Magn. Reson. **244**, 90 (2014).
[26]M. K. Pandey, M. Malon, A. Ramamoorthy, and Y. Nishiyama, J. Magn. Reson. **250**, 45 (2015).
[27]E. Salager, J.-N. Dumez, R. S. Stein, S. Steuernagel, A. Lesage, B. Elena-Herrmann, and L. Emsley, Chem. Phys. Lett. **498**, 214 (2010).
[28]R. Linser, M. Dasari, M. Hiller, V. Higman, U. Fink, J.-M. Lopez del Amo, S. Markovic, L. Handel, B. P. Schmieder, D. Oesterhelt, H. Oschkinat, and B. Reif, Angew. Chem., Int. Ed. **50**, 4508 (2011).
[29]G. P. Holland, Q. Mou, and J. L. Yarger, Chem. Commun. **49**, 6680 (2013).
[30]M. Huber, S. Hiller, P. Schanda, M. Ernst, A. Böckmann, R. Verel, and B. H. Meier, ChemPhysChem **12**, 915 (2011).
[31]V. Chevelkov, B. Habenstein, A. Loquet, K. Giller, S. Becker, and A. Lange, J. Magn. Reson. **242**, 180 (2014).
[32]E. Barbet-Massin, A. J. Pell, J. S. Retel, L. B. Andreas, K. Jaudzems, W. T. Franks, A. J. Nieuwkoop, M. Hiller, V. Higman, P. Guerry, A. Bertarello, M. J. Knight, M. Felletti, T. Le Marchand, S. Kotelovica, I. Akopjana, K. Tars, M. Stoppini, V. Bellotti, M. Bolognesi, S. Ricagno, J. J. Chou, R. G. Griffin, H. Oschkinat, A. Lesage, L. Emsley, T. Herrmann, and G. Pintacuda, J. Am. Chem. Soc. **136**, 12489 (2014).
[33]E. Barbet-Massin, M. Felletti, R. Schneider, S. Jehle, G. Communie, N. Martinez, M. R. Jensen, R. W. H. Ruigrok, L. Emsley, A. Lesage, M. Blackledge, and G. Pintacuda, Biophys. J. **107**, 941 (2014).
[34]M. J. Knight, I. C. Felli, R. Pierattelli, I. Bertini, L. Emsley, T. Herrmann, and G. Pintacuda, J. Am. Chem. Soc. **134**, 14730 (2012).
[35]A. Böckmann, M. Ernst, and B. H. Meier, J. Magn. Reson. **253**, 71 (2015).
[36]L. B. Andreas, T. Le Marchand, K. Jaudzems, and G. Pintacuda, J. Magn. Reson. **253**, 36 (2015).
[37]J. W. Traer, E. Montoneri, A. Samoson, J. Past, T. Tuherm, and G. R. Goward, Chem. Mater. **18**, 4747 (2006).
[38]R. Zhang, J. Damron, T. Vosegaard, and A. Ramamoorthy, J. Magn. Reson. **250**, 37 (2015).

[39]H. K. Miah, D. A. Bennett, D. Iuga, and J. J. Titman, J. Magn. Reson. **235**, 1 (2013).
[40]P. Paluch, T. Pawlak, J.-P. Amoureux, and M. J. Potrzebowski, J. Magn. Reson. **233**, 56 (2013).
[41]S. H. Park, C. Yang, S. J. Opella, and L. J. Mueller, J. Magn. Reson. **237**, 164 (2013).
[42]Y. Nishiyama, M. Malon, Y. Ishii, and A. Ramamoorthy, J. Magn. Reson. **244**, 1 (2014).
[43]R. Zhang, M. Pandey, Y. Nishiyama, and A. Ramamoorthy, Sci. Rep. **5**, 11810 (2015).
[44]T. Kobayashi, K. Mao, P. Paluch, A. Nowak-Król, J. Sniechowska, Y. Nishiyama, D. T. Gryko, M. J. Potrzebowski, and M. Pruski, Angew. Chem. **125**, 14358 (2013).
[45]R. Linser, B. Bardiaux, V. Higman, U. Fink, and B. Reif, J. Am. Chem. Soc. **133**, 5905 (2011).
[46]G. Bodenhausen, R. Freeman, and G. A. Morris, J. Magn. Reson. **23**, 171 (1976).
[47]H. Geen, X.-L. Wu, P. Xu, J. Friedrich, and R. Freeman, J. Magn. Reson. **81**, 646 (1989).
[48]A. E. Bennett, C. M. Rienstra, J. M. Griffiths, W. Zhen, P. T. Lansbury, and R. G. Griffin, J. Chem. Phys. **108**, 9463 (1998).
[49]Y. Ishii, J. Chem. Phys. **114**, 8473 (2001).
[50]G. Metz, X. L. Wu, and S. O. Smith, J. Magn. Reson., Ser. A **110**, 219 (1994).
[51]N. C. Nielsen, H. Bildso/e, H. J. Jakobsen, and M. H. Levitt, J. Chem. Phys. **101**, 1805 (1994).
[52]G. P. Holland, B. R. Cherry, J. E. Jenkins, and J. L. Yarger, J. Magn. Reson. **202**, 64 (2010).
[53]R. Zhang and A. Ramamoorthy, J. Magn. Reson. **243**, 85 (2014).
[54]L. Emsley and G. Bodenhausen, Chem. Phys. Lett. **165**, 469 (1990).
[55]M. Bak, J. T. Rasmussen, and N. C. Nielsen, J. Magn. Reson. **147**, 296 (2000).
[56]Z. Tošner, R. Andersen, B. Stevensson, M. Edén, N. C. Nielsen, and T. Vosegaard, J. Magn. Reson. **246**, 79 (2014).
[57]H. J. Simpson and R. E. Marsh, Acta Crystallogr. **20**, 550 (1966).
[58]K. Oda and H. Koyama, Acta Crystallogr., Sect. B: Struct. Sci. **B28**, 639 (1972).
[59]X. Wu and K. W. Zilm, J. Magn. Reson., Ser. A **104**, 154 (1993).
[60]A. Ramamoorthy, Y. F. Wei, and D.-K. Lee, Annu. Rep. NMR Spectrosc. **52**, 1 (2004).
[61]Y. F. Wei, D.-K. Lee, K. J. Hallock, and A. Ramamoorthy, Chem. Phys. Lett. **351**, 42 (2002).
[62]D. H. Zhou and C. M. Rienstra, Angew. Chem. **120**, 7438 (2008).
[63]Y. Nishiyama, T. Kobayashi, M. Malon, D. S. Arachchige, I. I. Slowing, and M. Pruski, Solid State Nucl. Magn. Reson. **66-67**, 56 (2015).
[64]K. Schmidt-Rohr, J. Clauss, and H. W. Spiess, Macromolecules **25**, 3273 (1992).
[65]Q. Chen and K. Schmidt-Rohr, Solid State Nucl. Magn. Reson. **29**, 142 (2006).
[66]M. J. Bayro, M. Huber, R. Ramachandran, T. C. Davenport, B. H. Meier, M. Ernst, and R. G. Griffin, J. Chem. Phys. **130**, 114506 (2009).